

# Electrohydrodynamics of cone-jet flow at high relative dielectric permittivity

A. V. Subbotin<sup>+1)</sup>, A. N. Semenov\*

<sup>+</sup>Topchiev Institute of Petrochemical Synthesis of the RAS, 119991 Moscow, Russia

\*Institut Charles Sadron, CNRS-UPR 22, Universite de Strasbourg, BP 84047, 67034 Strasbourg Cedex 2, France

Submitted 29 September 2015

Resubmitted 3 November 2015

In this paper we propose a new solution of the electrohydrodynamic equations describing a novel cone-jet flow structure formed at a conductive liquid meniscus in an electric field. Focusing on the liquids characterized by a high relative dielectric permittivity and using the slender body approximation, the cone-jet transition profiles and their characteristic radii are predicted in relation to the material parameters. The stable value of the cone angle is obtained using the Onsager's principle of maximum entropy production. Three different regimes of the cone-jet flow behavior are identified depending on the relative importance of capillary, viscous and inertial stress contributions. The presented complete analytical solutions for the cone-jet transition zone and the far jet region yield several different laws of algebraic decrease for the radius, surface charge and electric field of the jet.

DOI: 10.7868/S0370274X15240078

Electrohydrodynamic cone-jet structures appeared in electrospraying and electrospinning processes are of fundamental scientific interest [1, 2]. Theoretical analysis of these modes in steady-state is usually based on the Taylor's model of the conical features arisen on the surface of a conductive liquid meniscus when high electric potential is applied [3, 4]. Emanated from the cone apex a thin electrified jet is often treated using the slender body approximation [5, 6]. The static Taylor cone angle  $2\theta_c = 98.6^\circ$  has been calculated using the balance between the capillary and electrostatic forces and assumption on ideal conductivity of the liquid. According to the conventional point of view the conductive current dominates in the cone whereas the convective current dominates in the jet [7, 8]. The electric current along the cone-jet surface is usually disregarded without a solid justification [9, 10]. This assumption is lifted in the present study considering the cone-jet flow patterns in a liquid of high dielectric permittivity  $\varepsilon$ .

The basic electrohydrodynamic equations have been formulated in a scope of the leaky dielectric model [11]. Following this approach we assume a Newtonian liquid characterized by its density  $\rho$ , electrical conductivity  $K$ , viscosity  $\eta$ , and surface tension  $\alpha$ . For the surrounding gas medium  $\rho = K = 0$  and  $\varepsilon = 1$ . The conductivity  $K$  depends on the volume concentrations of positive

( $n_+$ ) and negative ( $n_-$ ) ions and their electrical mobilities  $\mu_+$ ,  $\mu_-$ ; the ions are monovalent with charge  $e$ , so  $K = e(n_+\mu_+ + n_-\mu_-)$ . Due to the electro-neutrality  $n_+ = n_- = n$ .

Let us consider a lower part of the cone (see Fig. 1) restricted by the basis of the radius  $r^\#$ . The total charge of positive ions in the bulk of the cone can be then estimated as  $\sim (\pi/3)enr^{\#3}/\tan\theta_c$ , where  $\theta_c$  is the semi-angle of the cone and  $r^\#/\tan\theta_c$  is its length. Concentration of the surface charge on the Taylor cone reads  $\sigma \sim (\alpha\varepsilon_0/r^\#)^{1/2}$  [1–3, 10]. Here  $\varepsilon_0$  is the dielectric permittivity of vacuum. Therefore, the total charge on the cone surface is  $\sim (4\pi/3)(\alpha\varepsilon_0)^{1/2}r^{\#3/2}/\tan\theta_c$ . Obviously, the surface charge exceeds the bulk charge for  $r^\# \leq r^* \sim 4(\alpha\varepsilon_0)^{1/3}(en)^{-2/3}$ . In this case the surface current in the cone/jet flow must exceed the conductive current in the bulk (if the cone/jet radius is smaller than  $r^*$ ). For example, a typical value of  $r^*$  for water could be estimated using the surface tension  $\alpha \approx 7.2 \cdot 10^{-2} \text{ N} \cdot \text{m}^{-1}$  and the concentration of positive ions  $n = 10^{-pH} \text{ mol/l}$  where  $\text{mol/l} = N_A/(10^3 \text{ cm}^3)$ . This gives  $n \approx 0.6 \cdot 10^{20} \text{ m}^{-3}$  and  $r^* \approx 75 \mu\text{m}$  for  $\text{pH} = 7$ . We expect that liquids with lower conductivity have larger  $r^*$  and addition of the salt decreases it value. Thus we arrive at the conclusion that the Taylor cone adjacent to the meniscus may fall into a new regime one its radius decreases below  $\sim r^*$ . It is the regime of dominant electric current along the surface that is considered below.

<sup>1)</sup>e-mail: subbotin@ips.ac.ru

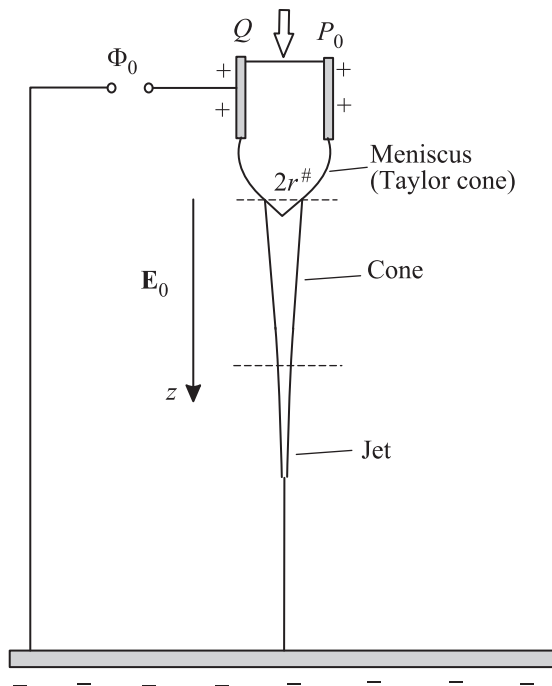


Fig. 1. A cone-jet structure formed in a liquid with high relative permittivity  $\varepsilon$ . The transition between the cone and the jet is smooth

As has been shown recently [9, 10] the conical structures different from the hydrostatic Taylor cone do emerge on the scales  $< r^*$ . Two families of the conical features are predicted there. The first family constitutes needle-like cones having a small apex angle,  $0 < \theta_c(\varepsilon) < 27^\circ$ ,  $\varepsilon > 1$ , tending to zero at  $\varepsilon \rightarrow \infty$ . The cones from the second family,  $36^\circ < \theta_c(\varepsilon) < 49.3^\circ$ ,  $\varepsilon > 12.6$ , have the apex angles close to the Taylor value  $2\theta_c = 98.6^\circ$  at  $\varepsilon \rightarrow \infty$ . In this paper we focus on the first family of conical structures for high relative dielectric permittivity ( $\varepsilon \gg 1$ ) giving rise to the highest electric current (presumably, these structures are the most stable). We consider the dynamics of the cone-jet flow generated by an electric field  $E_0$  (an external potential  $\Phi_0$ ) along the vertical  $z$ -axis, and by an external pressure  $P_0$  producing the flow rate  $Q$ . The relevant cone-jet geometry is shown in Fig. 1.

The cone and jet are supposed to be axially symmetric, so they are described by the radius  $r(z)$ . The flow is expected to be nearly uniform in the cross-section ( $z = \text{const}$ ) in the spirit of the slender body approximation since  $\theta_c \ll 1$  for  $\varepsilon \gg 1$ . So, the velocity  $v_z$  and the elongation rate  $dv_z/dz$  inside the cone-jet (generated by the external fields) are approximately given by

$$v_z \simeq \frac{Q}{\pi r^2(z)}, \quad \frac{dv_z}{dz} \simeq -\frac{2Qr'_z}{\pi z^3(z)}. \quad (1)$$

The momentum equation for the stationary regime in the framework of the slender body approximation ( $|r'_z| \ll 1$ ) reads [5, 6]

$$\frac{d}{dz} \left( \frac{\rho Q^2}{\pi^2 r^2} + \frac{6Q\eta}{\pi} \frac{d}{dz} \ln r \right) \simeq 2rF_\tau + r^2 \frac{d}{dz} (F_n - \alpha C). \quad (2)$$

Here  $C \simeq 1/r$  is the curvature of the surface. The components  $F_\tau$  and  $F_n$  of the electric force acting on the cone-jet surface are expressed via the tangential component of the electric field  $E_\tau$ , the total surface charge density  $\sigma = \sigma_c + \sigma_p$ , and the fraction of the conductive charge  $w = \sigma_c/\sigma$ , where  $\sigma_c$  and  $\sigma_p$  are the surface densities of the conductive and polarization charges correspondingly:

$$F_n = \frac{\sigma^2(\varepsilon - w^2)}{2\varepsilon_0(\varepsilon - 1)} + \frac{\varepsilon_0(\varepsilon - 1)E_\tau^2}{2}, \quad F_\tau = \sigma_c E_\tau, \quad (3)$$

The tangential electric field is a sum of the external field and the field created by the surface charges

$$E_\tau = E_0 \mathbf{e}_z \boldsymbol{\tau} + \frac{1}{4\pi\varepsilon_0} \text{P.V.} \int_{\tilde{A}} dA_1 \frac{\sigma(\mathbf{r} - \mathbf{r}_1) \boldsymbol{\tau}}{|\mathbf{r} - \mathbf{r}_1|^3}. \quad (4)$$

The total surface charge density  $\sigma$  is defined by the equation

$$\frac{\sigma(\varepsilon + 1 - 2w)}{2\varepsilon_0(\varepsilon - 1)} = E_0 \mathbf{e}_z \mathbf{n} + \frac{1}{4\pi\varepsilon_0} \text{P.V.} \int_{\tilde{A}} dA_1 \frac{\sigma(\mathbf{r} - \mathbf{r}_1) \mathbf{n}}{|\mathbf{r} - \mathbf{r}_1|^3} \quad (5)$$

which follows from the Coulomb's law [9, 10]. In (4), (5) P.V. implies the principle value, and integrations are performed over the cone-jet surface area  $\tilde{A}$ ;  $\boldsymbol{\tau}$  and  $\mathbf{n}$  are the tangential and normal unit vectors at the surface. Using the slender body approximation for Eq. (4), (5) and dividing the electric field into two parts one finds

$$E_\tau = E_z = E_{\text{near}} + E_{\text{far}}, \quad E_{\text{near}} = -\frac{\lambda}{\varepsilon_0} \frac{dq}{dz}, \quad (6)$$

$$\sigma_p = \sigma(1 - w) = -\frac{(\varepsilon - 1)\varepsilon_0}{2r} \frac{d}{dz} (r^2 E_z),$$

where  $\lambda = \ln \chi$ ,  $\chi = |r'_z|^{-1} = |dz/dr| \gg 1$  is the local aspect ratio,  $q = r\sigma$ . The electric field  $E_{\text{near}}$  is generated by the local charges ( $\Delta z < r\chi$ ) near the given surface point and  $E_{\text{far}}$  is the electric field generated by the distant parts ( $\Delta z > r\chi$ ) of the cone-jet and by the external potential.

The total electric current along the cone-jet surface is given by

$$I_0 = 2\pi r \sigma_c (v_\tau + \mu_+ E_\tau). \quad (7)$$

Here  $v_\tau$  is the tangential velocity of the flow on the surface. Generally,  $I_0$  includes the contribution generated

by the tangential electric traction which could exceed the velocity  $v_z$  due to the external flow [9, 10]. Here we neglect the conductive current in the bulk of the liquid  $\Delta I \simeq \pi r^2 K E_z$ :  $\Delta I$  is negligible in the cone-jet regions since their radii are assumed to be small,  $r \ll (\alpha \varepsilon_0)^{1/3} (\mu_+ / K)^{2/3} \sim r^*$ .

Let us consider the needle-like cone defined (for  $\varepsilon \gg 1$ ) by equation  $r(z) = -z \tan \theta_c \simeq -\theta_c z$  ( $z \leq 0$ ). We assume that the surface current is mainly driven electrically:  $v_z \ll \mu_+ E_z$ . This assumption is valid for  $r \gg a_1$ . It is analyzed and lifted below (see the text between Eqs. (13) and (14) including the definition of  $a_1$ ). On using the scaling behavior  $\sigma = A/\sqrt{r}$  in Eq. (6) ( $A = \text{const}$ ), and  $w = \text{const}$ , with  $r'_z \simeq -\theta_c$  we get (neglecting the contribution of the external field):

$$E_z \simeq \frac{A \theta_c \ln(1/\theta_c)}{2\varepsilon_0 \sqrt{r}}, \quad 1 - w \simeq \frac{3}{8}(\varepsilon - 1)\theta_c^2 \ln(1/\theta_c), \quad (8)$$

After substitution of  $E_z$  and  $\sigma_c$  in (7) one finds the relationship between the electric current and the parameter  $A$

$$I_0 \simeq \pi \mu_+ w A^2 \theta_c \ln(1/\theta_c) / \varepsilon_0. \quad (9)$$

Integrating Eq. (2) and applying (3) then gives

$$\frac{\rho Q^2}{\pi^2 r^2} + \frac{6Q\eta}{\pi} \frac{d}{dz} \ln r - \alpha r \simeq \simeq \frac{I_0 z}{\pi \mu_+} \left\{ 1 + \frac{1}{2w \ln(1/\theta_c)} \left[ 1 + \frac{\varepsilon}{4} \theta_c^2 \ln^2(1/\theta_c) \right] \right\}. \quad (10)$$

The viscous term in this equation can be neglected if  $r \gg (Q\eta\theta_c/\alpha)^{1/2}$ , while the inertial term is negligible if  $r \gg (\rho Q^2/\alpha)^{1/3}$ . Assuming both conditions which are valid if  $Q$  is low enough (the opposite regimes are discussed below, Eq. (13)) and recalling that  $r(z) \simeq -\theta_c z$  one gets the electric current as a function of the cone semiangle  $\theta_c$

$$I_0 \simeq \pi \mu_+ \alpha \theta_c \left\{ 1 + \frac{1}{2w \ln(1/\theta_c)} \left[ 1 + \frac{\varepsilon}{4} \theta_c^2 \ln^2(1/\theta_c) \right] \right\}^{-1}. \quad (11)$$

For  $\varepsilon \gg 1$  this equation is asymptotically equivalent to the general result obtained in [9, 10], however the flow regimes considered here and in Ref. [9, 10] are different. Here the flow is nearly uniform in the cross-section (by virtue of the slender body approximation) whereas in Ref. [9, 10] the flow pattern is more complicated, involving a considerable backflow nears the axis. By considering the hydrodynamic equations we established that the crossover between the two regimes is located at  $|z| \sim (Q\eta\theta_c/\alpha)^{1/2}/\theta_c = (Q\eta/\theta_c\alpha)^{1/2}$ . The important point is that both regimes correspond to the same cone geometry (with the same angle  $\theta_c$ ) in spite of the different flow patterns. The reason is simple: the flow field is

irrelevant as long as the cone shape is concerned since the viscous stress associated with the flow is negligible as compared with the capillary pressure.

The electric current and the cone semiangle  $\theta_c$  could be found after consideration of the full electrohydrodynamics of the meniscus and the meniscus/cone transition zone. However this difficult problem can be bypassed if we engage the Onsager's principle of maximum entropy production (MEP) which is well established for linear stationary processes [12–15]. More precisely, we employ the Onsager's variational principle in the generalized form due to Ziegler [16, 17]. This MEP principle says that if external forces acting on a nonequilibrium system are prescribed, the actual stationary state of the system maximizes the entropy production  $\dot{D}/T$  under the natural condition that the dissipated energy  $\dot{D}$  is balanced by the work  $W$  done on the system by external forces,  $\dot{D} = W$  [17]. In other words, a stable stationary process must maximize the work of external forces per unit time,  $W = \dot{D}$ . Many examples of the Onsager–Ziegler principle application, where the true regime is selected among an infinite family of possible nonequilibrium states, can be found in Refs. [14, 17]. In our case  $\dot{D} = \Phi_0 I_0 + P_0 Q$  depends on the cone angle  $\theta$ . Let us first omit the term  $P_0 Q$ . As far as the potential  $\Phi_0 = \text{const}$ , the maximum of entropy production corresponds to the maximum electric current. After maximization of the current (11) and using additionally the second Eq. (8) for  $w$  we arrive at the following results for the cone semiangle, the fraction of the mobile ions on the cone surface, the surface electric current, charge density and electric field:

$$\theta_c \simeq \frac{2}{\sqrt{3\varepsilon\lambda}}, \quad w \approx 0.5,$$

$$I_0 \simeq \pi \mu_+ \alpha g(\varepsilon), \quad g(\varepsilon) \simeq 0.75\theta_c,$$

$$A \simeq \left( \frac{3\alpha\varepsilon_0}{2\lambda r} \right)^{1/2}, \quad \sigma = \left( \frac{3\alpha\varepsilon_0}{2\lambda r} \right)^{1/2}, \quad E_z \simeq \left( \frac{\alpha}{2\varepsilon\varepsilon_0 r} \right)^{1/2}. \quad (12)$$

Here  $\lambda = \ln(1/\theta_c) \simeq 0.5 \ln \varepsilon$ . Now let us estimate the ratio  $P_0 Q / (\Phi_0 I_0)$ . The total applied voltage  $\Phi_0$  is higher than the electric potential difference  $\Delta\Phi$  between the cone section at the base,  $z = -z^\# = -r^\#/\theta_c$  (note,  $r^\# \sim r^*$ ), and the cone apex:  $\Phi_0 > \Delta\Phi$ . The difference  $\Delta\Phi$  can be estimated as  $\Delta\Phi \sim \int_{-z^\#}^0 E_z dz \sim E_z^\# z^\#$

where  $E_z^\# \sim \sqrt{\alpha/(\varepsilon\varepsilon_0 r^\#)}$ . The pressure  $P_0$  cannot exceed the pressure near the base of the cone  $P_0 < p^\# \sim \alpha/r^\#$  since the external pressure must not destroy the cone itself. Therefore,  $P_0 Q / (\Phi_0 I_0) < p^\# Q / (\Delta\Phi I_0) \simeq \simeq v_z^\# / (\mu_+ E_z^\#) \ll 1$ . Here we use the estimation  $I_0 \simeq$

$\simeq \mu_+ \alpha \theta_c$  and  $v_z^\# \simeq Q/(\pi r^{\#2})$ . Thus, the term  $P_0 Q$  can be neglected and the optimum angle and the electric current are correctly defined in Eq. (12). Note that the electrified jet just slightly affects the above estimations, so it could be disregarded at this stage. In addition, at the meniscus/cone transition zone ( $\sim r^*$ ) the conductive current is  $\Delta I \sim I_0$ .

The thickness  $\delta$  of the surface charge layer in the cone could be found from the relation  $eE_n \delta \simeq k_B T$ , where  $k_B$  is the Boltzmann constant,  $T$  is the temperature, and  $E_n \simeq \frac{1}{\varepsilon} \left( \frac{\alpha}{\varepsilon_0 r} \right)^{1/2}$  is the normal component of the electric field:  $\delta \simeq \frac{k_B T \varepsilon}{e} \left( \frac{\varepsilon_0 r}{\alpha} \right)^{1/2}$ . Of course, it is necessary to demand that the charged layer is thin:  $\delta \ll r$  which is equivalent to

$$r \gg r_{\min} = l_0^3 / l_B^2, \quad (13)$$

where  $l_B = \frac{e^2}{4\pi\varepsilon_0 k_B T}$  is the Bjerrum length, and  $l_0 = \left( \frac{e^2}{\varepsilon_0 \alpha} \right)^{1/3}$  is the microscopic capillary length. Obviously,  $\delta$  is much smaller than the Debye radius  $r_D \simeq \left( \frac{\varepsilon \varepsilon_0 k_B T}{e^2 n} \right)^{1/2}$ :  $\delta \ll r_D$  since  $\sigma \simeq \sigma_c \gg en\delta$  (the latter condition is ensured by the surface current dominance,  $r \ll r^*$ , and by the condition (13)).

The conical structure fails at the apex once the inertial or viscous terms in Eq. (10) become dominant, or when the convection becomes faster than the electrical drift,  $v_z = \frac{Q}{\pi r^2(z)} \geq \mu_+ E_z$ . This transition can be described in terms of three characteristic radii defining the cone-jet transformation region. They correspond to three distinct flow regimes. In the regime I the conical structure is changed when the surface current starts to be governed by the flow convection, i.e. when  $v_z = \frac{Q}{\pi r^2} \simeq \mu_+ E_z$ . The electric field in the cone is given by  $E_z \simeq \left( \frac{\alpha}{2\varepsilon \varepsilon_0 r(z)} \right)^{1/2}$ , therefore, the radius of the cone-jet transition zone is  $r(z) \simeq a_1 = \left( \frac{2Q^2 \varepsilon \varepsilon_0}{\pi^2 \mu_+^2 \alpha} \right)^{1/3}$ . In the regime II the cone-jet transition is initiated by inertia once  $\rho v_z^2 \simeq \frac{\alpha}{r(z)}$ . The corresponding radius of the transition zone reads  $r(z) \simeq a_2 = \left( \frac{\rho Q^2}{\pi^2 \alpha} \right)^{1/3}$ . Finally, the cone-jet transition in the regime III occurs when the viscous force is of the order of the capillary force,  $\frac{6Q\eta}{\pi r^3(z)\sqrt{\varepsilon}} \simeq \frac{\alpha}{r(z)}$ . This condition leads to the radius  $r(z) \simeq a_3 = \left( \frac{6Q\eta}{\pi \alpha \sqrt{\varepsilon}} \right)^{1/2}$ . The cone-jet transition zone, which depends on the regime, can be defined as  $-z_i \leq z \leq z_i = a_i / \theta_c$ ,  $i = 1, 2, 3$ . It is important to note that in the regimes II and III the inequality  $v_z \ll \mu_+ E_z$  remains valid also right outside the cone-jet transition zone.

Let us first consider the regime I implying that  $a_1 > \max(a_2, a_3)$ . In the transition/jet region the electric field is  $E = E_{\text{far}} + E_{\text{near}}$  (cf. Eq. (6)). Here the transition zone is defined by the condition  $E_z \sim \tilde{Q}/r^2$ , where  $\tilde{Q} = Q/(\pi \mu_+)$ . The electric field generated by the cone ( $-\infty < z < 0$ ) along the  $z$ -axis in the jet region ( $z > z_1$ ) is found from the second term in the r.h.s. of Eq. (4),

$$E_{\text{far}}(z) \simeq \frac{\pi}{4} \left( \frac{3\alpha\theta_c}{2\varepsilon_0 \lambda z} \right)^{1/2}. \quad (14)$$

The local contribution in the electric field  $E_{\text{near}}$ , is defined in Eq. (6) where the surface contribution of mobile ions is (cf. Eq. (7)):

$$\sigma_c = \frac{\alpha g(\varepsilon)}{2r(E_z + \tilde{Q}/r^2)}. \quad (15)$$

In the transition zone  $E_{\text{near}}$  exceeds  $E_{\text{far}}$  by a factor  $\lambda$ :  $E_{\text{near}} \gg E_{\text{far}}$ , therefore  $E_{\text{far}}$  can be neglected there. The full set of equations in this case reads

$$q = q_c + q_p, \quad q_c \simeq \frac{\alpha g(\varepsilon)}{2E_z(1 + \tilde{Q}/r^2)}, \quad q_p \simeq -\frac{\varepsilon}{2} \frac{d}{dz}(r^2 E_z), \quad (16a)$$

$$-\alpha \frac{dr}{dz} \simeq 2rF_\tau + r^2 \frac{dF_n}{dz}. \quad (16b)$$

Here  $rF_\tau \simeq q_c E_z$  and  $F_n \simeq \varepsilon \varepsilon_0 E_z^2/2$  (the  $\sigma^2$  contribution is neglected since  $\sigma^2/(\varepsilon \varepsilon_0^2 E_z^2) \sim 1/\lambda$  in the transition zone). After some transformations and reduction

$$\bar{r} = r/a_1, \quad \bar{z} = z/z_1, \quad \bar{E} = E/E^*, \quad \bar{q} = q/q^*, \quad (17a)$$

$$E^* = \left( \frac{\alpha}{2\varepsilon \varepsilon_0 a_1} \right)^{1/2}, \quad q^* = \alpha g(\varepsilon)/E^* \quad (17b)$$

the following system is obtained:

$$\frac{d\bar{E}}{d\bar{z}} = -\frac{3}{2} \frac{1}{1 - \bar{E}^2 \bar{r}} \left( \frac{2\bar{q}}{\bar{z}^2} - \frac{1 + \bar{E}^2 \bar{r}}{1 + \bar{E}^2 \bar{r}} \right) \quad (18a)$$

$$\frac{d\bar{q}}{d\bar{z}} = -\frac{\bar{E}}{2}, \quad \frac{d\bar{r}}{d\bar{z}} = \frac{3}{2} \frac{\bar{E}}{1 - \bar{E}^2 \bar{r}} \left( \bar{q} - \frac{1}{\bar{E} + \bar{r}^{-2}} \right). \quad (18b)$$

These equations can be solved numerically (assuming conjugation with the cone, i.e.  $\bar{r} \simeq |\bar{z}|$  at  $z \rightarrow -\infty$ , etc.). The result is shown in Fig. 2. The fraction of the conductive charge  $\bar{w} \simeq \frac{0.5}{\bar{q}(\bar{E} + \bar{r}^{-2})}$  changes from 0.5 to 1 in the transition zone. At  $\bar{z} \gg 1$ ,  $\bar{E}$  vanishes exponentially,  $\bar{E} \propto e^{-1.3\bar{z}}$ , while  $\bar{q} \rightarrow \bar{q}_0 = 1$  and  $\bar{r} \rightarrow \bar{r}_0 = \sqrt{2}$ .

Having analyzed the very cone-jet transition zone ( $z \sim z_1$ ), we can now take into account the field  $E_{\text{far}}$ , which is relevant for  $z \gg z_1$ . In this region  $\bar{E} \simeq \bar{E}_{\text{far}} \ll 1$ ,  $q \gg q_p$ , so Eqs. (18a) and (18b) can be simplified as

$$\bar{q} \simeq \bar{r}^2/2, \quad \frac{d\bar{r}}{d\bar{z}} \simeq -\frac{3}{4} \bar{E} \bar{r}^2, \quad (19)$$

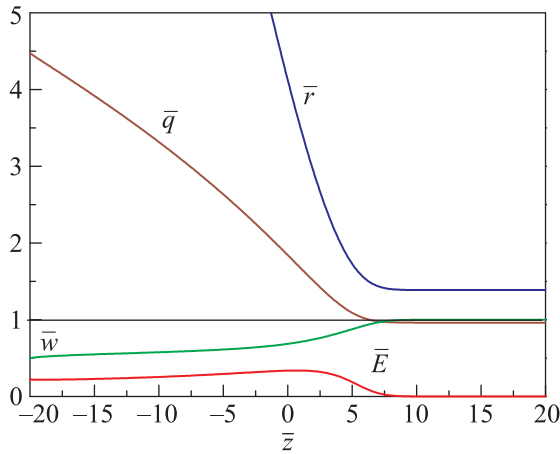


Fig. 2. (Color online) The non-dimensional radius of the cone-jet  $\bar{r}$ , the surface charge density  $\bar{q}$ , the tangential electric field  $\bar{E}$  and the fraction of the surface ions  $\bar{w}$ , as functions of the reduced coordinate  $\bar{z}$

where  $\bar{E} \simeq \bar{E}_{\text{far}} \frac{\pi}{2\lambda} \bar{z}^{-1/2}$ . Taking the plateau values  $\bar{q}_0 = 1$  and  $\bar{r}_0 = \sqrt{2}$  as initial conditions for Eqs. (19), we get

$$\bar{r} \simeq \frac{\sqrt{2}}{1 + k\sqrt{\bar{z}}}, \quad \bar{q} \simeq (1 + k\sqrt{\bar{z}})^{-2}, \quad k \equiv \frac{3\pi\sqrt{2}}{4\lambda}, \quad z \gg z_1. \quad (20)$$

It gives the second transition scale  $z_1^* = z_1/k^2 \sim z_1\lambda^2$ . These results provide the complete description of the cone-jet transition zone.

The jet profile in the zone  $z_1^* < z < z^\#$  can be found from Eq. (2) taking into account that the normal electric traction is negligible,  $F_n \simeq \frac{\sigma^2}{2\varepsilon_0} + \frac{\varepsilon\varepsilon_0 E_z^2}{2} \simeq \frac{\alpha r^2(z)}{a_1^3} + \frac{\alpha\sqrt{\varepsilon}}{2z} \ll \ll \frac{\alpha}{r(z)}$ , and  $E_z \simeq E_{\text{far}} \propto z^{-1/2}$  (cf. Eq. (14)):

$$\begin{aligned} \frac{d}{dz} \left( \frac{\rho Q^2}{\pi^2 r^2} + \frac{6Q\eta}{\pi} \frac{d}{dz} \ln r - \alpha r \right) &\simeq \\ &\simeq \alpha g(\varepsilon) \left( 1 + \frac{\tilde{Q}}{E_z r^2(z)} \right)^{-1}. \end{aligned} \quad (21)$$

The above equation readily gives the following profiles

$$r \simeq a_1 \left( \frac{2z_1^*}{z} \right)^{1/2}, \quad z_1^* < a < \tilde{z}_1 = z_1^* \left( \frac{a_1}{a_2} \right)^2, \quad (22a)$$

$$r \simeq a_2 \left( \frac{\tilde{z}_1}{z} \right)^{1/8}, \quad \tilde{z}_1 < z < z^\#. \quad (22b)$$

The regime, Eq. (22a), results from the competition between the capillary force and electrical traction. In the second regime, Eq. (22b), the capillary force is dominated by inertial effects. The scaling dependence  $r \propto z^{-1/8}$  in the jet was predicted in Ref. [7] for an entirely different regime of an inviscid flow in a perfectly

conducting liquid. Note that the viscous term is always relatively small.

At  $z > z^\#$  the electric field is nearly constant and is determined by the external potential, therefore the profile is [5]

$$r \simeq a_2 \left( \frac{\tilde{z}_1}{z} \right)^{1/8} \left( \frac{z^\#}{z} \right)^{1/4}, \quad z > z^\#. \quad (22c)$$

In the regimes II and III the inequality  $\frac{\tilde{Q}}{\pi r^2(z)} \ll E_z$  is fulfilled right outside the cone-jet transition zone, and the electric field is mainly determined by the neighboring part of the jet:  $E_z \simeq E_{\text{near}}$ . The polarization charge can be also neglected in this case, so the surface charge density  $\sigma \simeq \sigma_c \simeq \alpha g(\varepsilon)/(2rE_z)$ . Using (6) we find an equation on  $E_z$ :

$$E_z \simeq -\frac{\lambda\alpha g(\varepsilon)}{2} \frac{d}{dz} \left( \frac{1}{E_z} \right). \quad (23)$$

This equation always leads to a singularity of the electric field at a finite  $z$  (on a scale  $\sim \max(z_2, z_3)$ ), and, therefore, to a divergence of the normal electric traction  $F_n \sim \varepsilon\varepsilon_0 E_z^2$  which cannot be balanced by the capillary pressure. It suggests an inherent instability of the straight jet in the regimes II and III.

In summary, we have explored a novel type of self-similar needle-like conical features arisen on the liquid meniscus dwelled in the electric potential. We have shown that the cone transforms to the straight jet if the imposed flow rate  $Q > \frac{54\pi\eta^3\mu_+^4}{\varepsilon^{7/2}\varepsilon_0^2\alpha}$  and  $\varepsilon > \frac{\rho\mu_+^2}{2\varepsilon_0}$ . Otherwise a jet formation is impossible due to a singularity of the electric field generated by the cone-jet conductive flow. Presumably, a droplet plume [18] should be formed in the latter case. This issue requires a further consideration. We predict that the cone apex angle scales as  $\theta_c \sim \varepsilon^{-1/2}$  and that the jet radius decreases first as  $z^{-1/2}$ , then as  $z^{-1/8}$  and finally as  $z^{-1/4}$  at the largest distance  $z$  from the cone apex which is in a good agreement with the measured jet radius behavior [19, 20]. Note that the scaling regime  $r \propto z^{-1/2}$  is obtained here for a jet of a simple Newtonian liquid as opposed to the results of Refs. [20, 21] where the same scaling law was established in a different regime for a complex viscoelastic liquid. The electric current carried by the cone-jet surface  $I_0 \sim \mu_+ \alpha \varepsilon^{-1/2}$  increases with increasing the surface tension and decreases with increasing the dielectric constant of the liquid. It does not depend on the flow rate  $Q$  as long as it low enough,  $Q < \left( \frac{\alpha\mu_+^2 r^\#^3}{\varepsilon\varepsilon_0} \right)^{1/2}$ .

Experimental investigation of the proposed cone-jet structures is one of the challenging problems. Presumably such structures could be identified in a number

of high-speed photographs of the electrospinning process [20, 22]. The transverse oscillatory movement of the tracer particles observed in the onset of the jet and attributed to the vortex flow field in the cone predicted in Refs. [10, 11] confirms the above assumption.

A.V.S. acknowledges financial support from the Russian Foundation for Basic Research (Grant #14-03-00299a).

- 
1. J. Fernández de la Mora, *Ann. Rev. Fluid Mech.* **39**, 217 (2007).
  2. D.H. Reneker, A.L. Yarin, E. Zussman, and H. Xu, *Adv. Appl. Mech.* **41**, 43 (2007).
  3. G.I. Taylor, *Proc. R. Soc. Lond. A* **280**, 383 (1964).
  4. R.T. Collins, J.J. Jones, M.T. Harris, and O.A. Basaran, *Nat. Phys.* **4**, 149 (2008).
  5. N. Kirichenko, I.V. Petryanov-Sokolov, N.N. Suprun, and A.A. Shutov, *Sov. Phys. Dokl.* **31**, 611 (1986).
  6. J.J. Feng, *Phys. Fluids* **14**, 3912 (2002).
  7. A.M. Gañán-Calvo, *Phys. Rev. Lett.* **79**, 217 (1997).
  8. F.J. Higuera, *J. Fluid Mech.* **484**, 303 (2003).
  9. A.V. Subbotin, *JETP Lett.* **100**, 657 (2014).
  10. A.V. Subbotin and A.N. Semenov, *Proc. R. Soc. Lond. A* **471**, 20150290 (2015).
  11. D.A. Saville, *Annu. Rev. Fluid Mech.* **29**, 27 (1997).
  12. L. Onsager, *Phys. Rev.* **37**, 405 (1931).
  13. L. Onsager and S. Machlup, *Phys. Rev.* **91**, 1505 (1953).
  14. M. Doi, *J. Phys.: Cond. Mat.* **23**, 284118 (2011).
  15. P. Županović, D. Kuić, Ž.B. Lovsić, D. Petrov, D. Jurčić, and M. Brumen, *Entropy* **12**, 996 (2010).
  16. H. Ziegler, in: *Progress in Solid Mechanics*, ed. by I.N. Sneddon and R. Hill, North-Holland, Amsterdam (1963), v. 4.
  17. L.M. Martyushev and V.D. Seleznev, *Phys. Rep.* **426**, 1 (2006).
  18. Y. Wang, M.K. Tan, D.B. Go, and H.-C. Chang, *Europhys. Lett.* **99**, 64003 (2012).
  19. I. Greenfeld, K. Fezzaa, M.H. Rafailovich, and E. Zussman, *Macromolecules* **45**, 3616 (2012).
  20. M.E. Helgeson, K.N. Grammatikos, J.M. Deitzel, and N.J. Wagner, *Polymer* **49**, 2924 (2008).
  21. A. Subbotin, R. Stepanyan, A. Chiche, J.J.M. Slot, and G. ten Brinke, *Phys. Fluids* **25**, 103101 (2013).
  22. L.M. Bellan, H.G. Craighead, and J.P. Hinstroza, *J. Appl. Phys.* **102**, 094308 (2007).